

# Seismic performance of dual frames with composite CF-RHS high strength steel columns



**C. Vulcu, A. Stratan, D. Dubina & S. Bordea**

*Department of Steel Structures and Structural Mechanics,  
Politehnica University of Timisoara, Timisoara, Romania*

## SUMMARY:

The paper summarizes the work carried out with the aim to investigate and evaluate the seismic performance of dual-steel building frames. The frames are considered to be dual eccentrically braced frames (D-EBF) and dual buckling restrained braced frames (D-BRBF). For the D-EBF, short as well as intermediate length links were considered. The investigated frames are realized as dual-steel frames in which mild carbon steel (MCS) is used in dissipative members while high strength steel (HSS) is used in non-dissipative “elastic” members. Therefore, the beams in MRF and dissipative links in EBF are realized of S355 steel grade, while the columns are concrete filled rectangular hollow section tubes (CF-RHS) of high strength steel (S460 and S700). Moment resisting joints are of welded connection in two different typologies: with reduced beam section (RBS) and with cover plates (CP). The specific detailing for these two solutions is displayed. The design of the frames was performed according to provisions from the seismic design code (EN 1998), with the aim to keep the columns in the elastic range up to the ultimate limit state. The moment-rotation relationship of the joints was obtained with an advanced FE model calibrated via experimental results. The seismic performance of the frames was evaluated through incremental dynamic analysis (IDA). Finally, results and conclusions are displayed with regard to failure mechanism and damage localization.

*Keywords: Dual-Steel Frames, High Strength Steel, Concrete Filled Tubes (CFT)*

## 1. DESIGN OF FRAMES AND JOINTS

### 1.1. Design of frames

In the framework of a European research project (HSS-SERF), which aims at investigating and evaluating the seismic performance of dual-steel building frames, two specific topologies of welded connections are studied. The interest for the study of the joints is to assess the overstrength contribution of the MRF to EBF for which the short links evidence yielding even at serviceability limit state. To evaluate seismic behaviour, a parametric study was carried out varying soil type (stiff and soft soil) and steel grade (S460 and S700), see Table 1. Fig. 1 illustrates the three frame typologies which were designed in accordance with EN 1998-1 (2004). The frames have 28 m height with 8 storeys of 3,5 m height and 3 bays of 7,5 m span. The external bays are moment resisting and the central bay is eccentrically braced containing short links (Fig. 1a), eccentrically braced with intermediate links (Fig. 1b), and buckling restrained (Fig. 1c). The beams are realized from mild carbon steel (S355), and the columns from high strength steel tubes (S460 and S700) filled with C30/37 concrete. A permanent load of 4 kN/m<sup>2</sup> and a live load of 3 kN/m<sup>2</sup> were used in the design. It was considered that the frames are located in a zone with peak ground acceleration equal to 0,32g. The linear analysis was carried out through modal response spectrum analysis. The design spectrum for stiff soil and soft soil, used for dual-eccentrically braced frames and dual concentrically braced frames with buckling restrained braces, was obtained considering a behaviour factor equal to 6. The stiff soil was considered to be type C according to EN 1998-1 (2004), while the response spectrum for soft soil (typical in Bucharest, Romania) was considered according to P100-1(2006). The beams from MRF system were designed from the fundamental load combination obtaining the same cross section for all

storeys (IPE400). The columns from 5<sup>th</sup> to 8<sup>th</sup> floor were designed with S355 steel grade. If designed with HSS, the cross-section of the columns would be smaller and would not allow manufacturing the connection with the beams. The short links have a 0.5 m span, and the intermediate length links a 0.9 m span. Table 1.2, Table 1.3 and Table 1.4 summarize the cross sections of the members obtained from the design of the three investigated frame configurations.

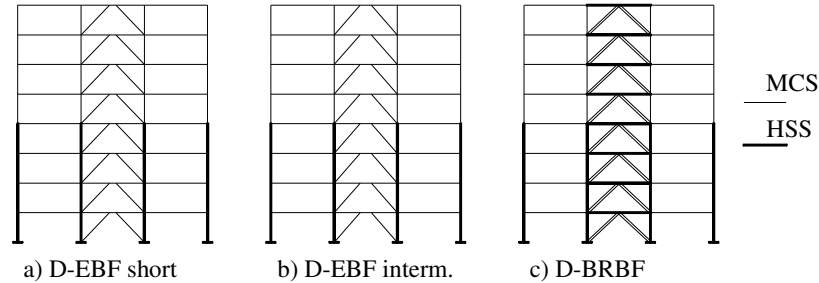


**Figure 1.** Investigated frame typologies

**Table 1.1.** Definition of frame configurations for parametric study

Frame	1	2	3	4	5	6	7	8
HSS	S460		S460		S700		S700	
Soil	Stiff		Soft		Stiff		Soft	
Joint	RBS	CP	RBS	CP	RBS	CP	RBS	CP

**Table 1.2.** Inner beams (links) within D-EBF's, and BRB within D-BRBF's:

Storey	Inner beams (links) in frame configuration:				BRB in:	
	D-EBF short		D-EBF intermediate		D-BRBF	
	1-2-5-6	3-4-7-8	1-2-5-6	3-4-7-8	Cross-section (txb)	
8	IPE 240	IPE 240	IPE 240	IPE240	15x30	25x30
7	IPE 240	IPE 270	IPE 240	IPE300	20x40	30x40
6	IPE 240	IPE 300	IPE 240	IPE360	25x40	35x50
5	IPE 270	IPE 360	IPE 270	IPE360	30x40	40x55
4	IPE 270	IPE 360	IPE 270	IPE360	30x40	45x50
3	IPE 300	IPE 400	IPE 270	IPE400	30x45	45x55
2	IPE 300	IPE 400	IPE 300	IPE400	30x50	50x60
1	IPE 300	IPE 400	IPE 270	IPE360	35x40	45x55

**Table 1.3.** Members within D-EBF short and D-EBF intermediate:

Frame config.	Columns		MRF beams
	Ground to 4 <sup>th</sup> floor	5 <sup>th</sup> to 8 <sup>th</sup> floor	
1-2	SHS 400x16 - S460	SHS 300x8 - S355	IPE 400
3-4	SHS 400x16 - S460	SHS 300x8 - S355	IPE 400
5-6	Box 325x12 - S700	SHS 300x8 - S355	IPE 400
7-8	Box 350x14 - S700	SHS 300x8 - S355	IPE 400

**Table 1.4.** Members within D-BRBF:

Frame config.	Columns		MRF beams
	Ground to 4 <sup>th</sup> floor	5 <sup>th</sup> to 8 <sup>th</sup> floor	
1-2	SHS 400x16 - S460	SHS 300x10 - S355	IPE 400
3-4	Box 400x20 - S460	SHS 300x10 - S355	IPE 400
5-6	Box 340x16 - S700	SHS 300x10 - S355	IPE 400
7-8	Box 350x16 - S700	SHS 300x10 - S355	IPE 400

## 1.2. Design of joints

Two joint typologies, reduced beam section (RBS) and cover plate (CP) beams are welded to columns in order to obtain ductile and over-strength joints, according to EN 1998-1 (2004) request. The connection solution is based on an outer diaphragm welded around the steel tube (see Fig. 2 and Fig. 3). The design of the joints was performed considering plastic hinge formation in the beams. The other components of the connection (welded on-site connection, stiffeners and column panel) were designed so as to reach a higher resistance than the beam. The resistance of the column panel in shear was checked based on provisions within EN 1998-1 (2004) and EN 1994-1 (2004) design codes. The transformation factor was considered to have a value of  $\beta=1$  due to the fact that the bending moment acts only from one side of the joint.

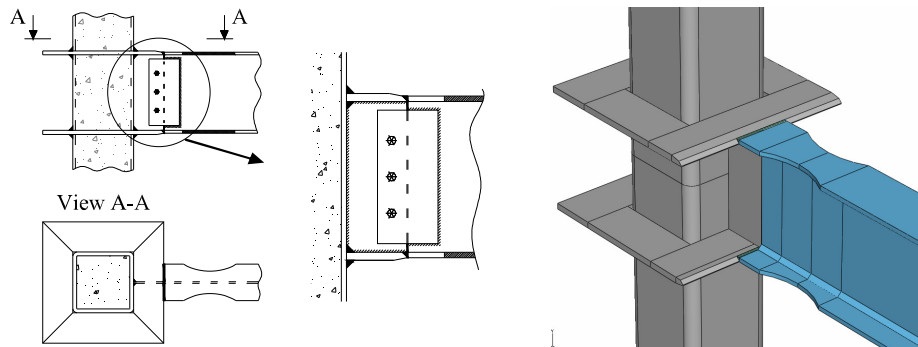


**Figure 2.** Joint with reduced beam section (RBS)

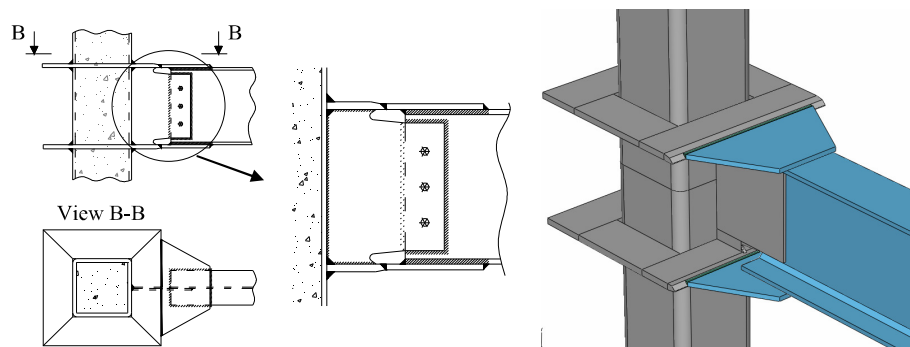


**Figure 3.** Joint with cover plates (CP)

## 2. NUMERICAL INVESTIGATION OF THE BEAM-TO-COLUMN JOINTS

### 2.1. Description of the numerical model

With the aim of assessing the behaviour of the two joints under cyclic loading, a set of numerical simulations have been performed with the finite element modelling software Abaqus (2007). The numerical models of the joint configurations contained: concrete filled tube (C30/37), column stiffeners (S460 plates of 20 mm thickness and 150 mm width), beam (IPE 400 S355) and cover plates (S355 steel grade of 15 mm thickness and 500 mm width). All the components of the joints were modelled using solid elements. The engineering stress-strain curves of the steel grades were obtained from the steel producers. The material model was therefore calibrated based on results from tensile tests, as shown in the work of Vulcu et. al. (2012). For the concrete core, a damaged plasticity model was used, as explained by Korotkov et. al. (2004). A dynamic explicit type of analysis was used, and for the interaction between the steel tube and the concrete core, a normal contact was defined. The load was applied through displacement control at the tip of the beam. The mesh of the elements was done using linear hexahedral elements of type C3D8R.

## 2.2. Calibration of the numerical models

The numerical models of the designed joints were calibrated based on results from the literature considering similar joint configurations. The work of Park et al. (2005) was considered for this purpose. Full-scale joint sub-assembly tests were conducted to assess the cyclic performance of wide flange beams to square CFT column joints reinforced with stiffening plates. Specimen B3 was chosen for the calibration of the numerical model. Information about the joint configuration, geometry and material can be found in the mentioned paper. The same modeling procedures were used, as presented above. For the material model of the steel grade, three cases were investigated, i.e. material with isotropic hardening, material with kinematic hardening as well as material with combined isotropic/kinematic hardening. The best results were obtained using the combined isotropic/kinematic hardening model, containing the cyclic hardening parameters from Dutta et. al. (2010). Fig. 4 shows the stress distribution, the plastic strain and the comparison between test and simulation in terms of moment-rotation curve.

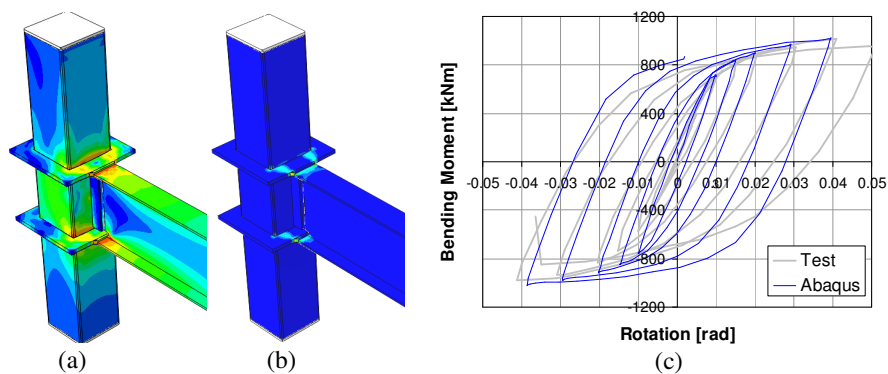


Figure 4. von Mises stress distribution (a), equiv. plastic strain (b) and moment rotation curve (c)

## 2.3. Cyclic behaviour of the beam-to-column joints

The calibration of the numerical model of the joint – including the material model and the cyclic loading procedure - allowed assessing the behavior to cyclic loading of the beam-to-column joints (RBS and CP). The cyclic analysis was performed using a loading procedure characterized by 5 complete cycles with a smooth shape as shown in Fig. 5.

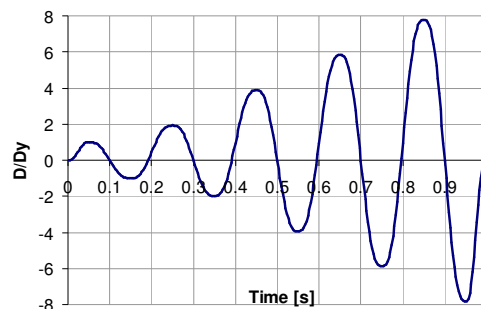


Figure 5. Cyclic loading procedure

The amplitudes in the first cycle correspond to the yield displacement ( $D_y$ ) from the monotonic analysis (the corresponding yield rotation is 0.015 rad for the RBS joint and 0.019 rad for the CP joint). The amplitudes in the next four cycles correspond to  $2D_y$ ,  $4D_y$ ,  $6D_y$  and  $8D_y$  respectively. The hysteretic loops characterizing the response to cyclic loading are shown in Fig. 6 and Fig. 7 for the joint with reduced beam section and respectively joint with cover plates. It can be observed that large plastic deformations occurred, for both joints, in the beam. Therefore, the main source of ductility is given by the plastic hinge in the beam. The two numerical models of the joints exceeded a rotation of

0.1 rad. Under a loading procedure demanding in low cycle fatigue (i.e. the ECCS loading procedure characterized by three cycles per amplitude) it is expected to achieve experimentally a maximum rotation of 0.05 rad. The beam has the same cross section for both joints. Therefore, the difference in behaviour is given by the reduction of the beams cross-section in the case of the RBS joint.

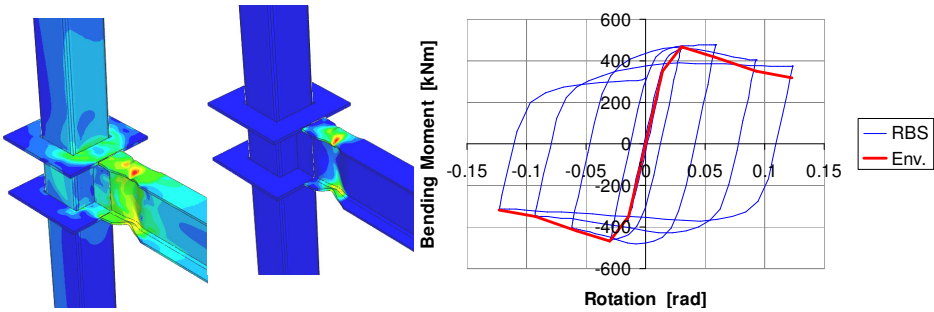


Figure 6. Cyclic response of the joint with reduced beam section

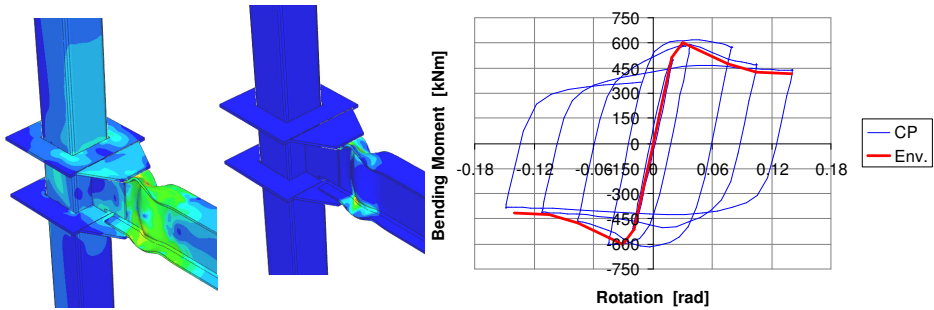


Figure 7. Cyclic response of the joint with cover plates

### 3. SEISMIC PERFORMANCE EVALUATION

#### 3.1. Frame modelling procedure

The modelling of the structures was performed using SAP2000 (2010). The joints within the moment resisting bays were modelled using short “nl-link” elements. The results from the cyclic analysis of the joints, i.e. the envelope of the hysteretic loops, were assigned to the “nl-link” element neglecting the elastic branch of the moment rotation curve and considering a kinematic behaviour. The P-Delta effect of the seismic mass that is not tributary to the frame was considered employing a leaning column. Fig. 8a illustrates the inelastic model used for the buckling restrained braces. This model was calibrated by Bordea (2010) based on extensive experimental tests performed on buckling restrained braces.

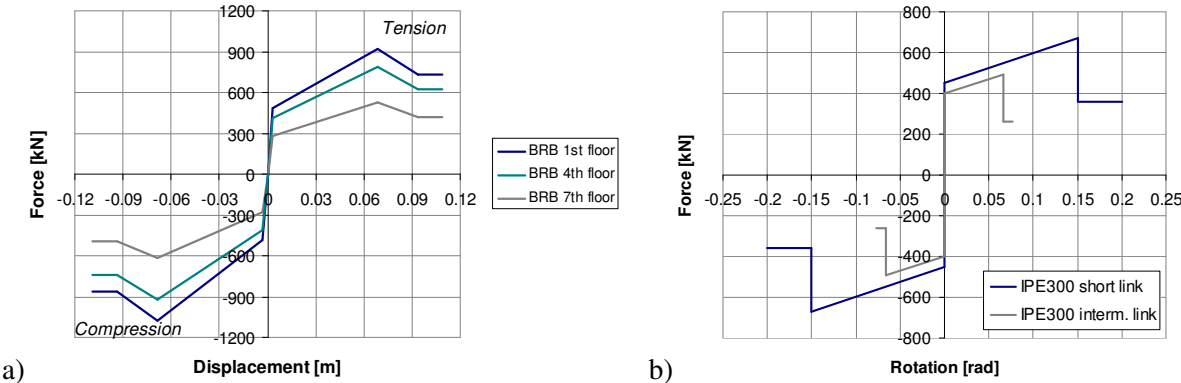


Figure 8. Inelastic model for BRB a), and links b)

Fig. 8b illustrates the modelling procedure used for short and intermediate length links of the D-EBF. The acceptance criteria used for short and intermediate length links, as well as for BRB was based on FEMA 356 (2000).

### 3.2. Pushover analysis

Pushover analyses were performed in order to assess the inelastic behaviour of the frames. With this type of analysis it is possible to identify the critical regions, the sequence of yielding, failure of structural components and the progress of the overall capacity curve of the structure.

Within the pushover analyses, the lateral storey forces were assumed to be proportional to the 1<sup>st</sup> mode. For each of the three frame configurations shown in Fig. 1, five cases were investigated, i.e. dual-frame with cover plate (CP) joints in the MRF bays, dual-frame with reduced beam section (RBS) joints in the MRF bays, standard frame (EBF, or BRBF) with pinned beams in the MRF bays, MRF with CP joints and pinned links in the EBF bay, and MRF with RBS joints and pinned links in the EBF bay. The capacity curves, in terms of base shear versus global drift angle, corresponding to the cases described above are shown in Fig. 9 to Fig. 11. Immediate occupancy, life safety and collapse prevention performance levels were marked on the capacity curves of dual frames. Fig. 9 shows the pushover curves for the D-EBF designed for stiff soil, in one case with short links and in the other case with intermediate length links. Based on the cross sections obtained from design, the intermediate length links are closer to long links and therefore the parameters used for the link model (i.e. maximum rotation) are significantly lower than those related to short links (Fig. 8b). As a result, the lateral deformation and base shear force are lower compared to the D-EBF with short links.

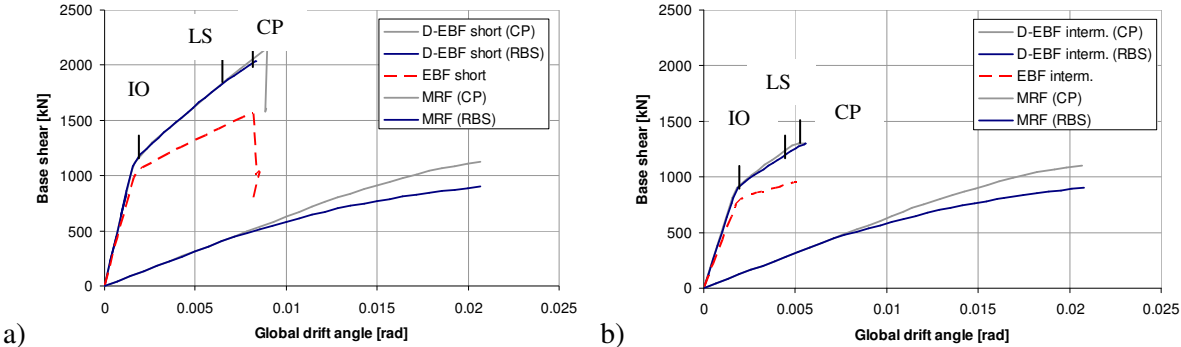


Figure 9. Pushover curves of D-EBF designed for stiff soil: a) with short links, and b) with intermediate links

Fig. 10 shows the comparison between the D-EBF with short links and D-EBF with intermediate links designed for soft soil. Based on the cross sections obtained from design, in this case the intermediate length links are closer to short links and therefore the capacity curves are similar, with the difference that the D-EBF with intermediate length links is characterised by a higher flexibility.

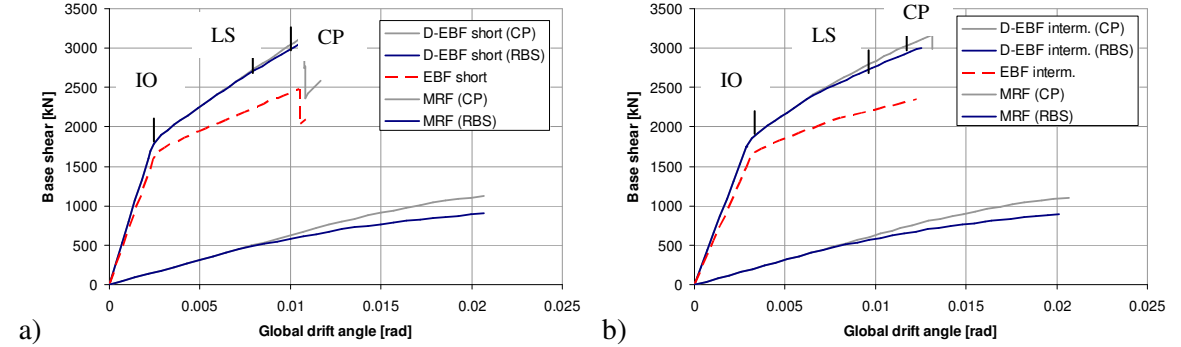


Figure 10. Pushover curves of D-EBF designed for soft soil: a) with short links, and b) with intermediate links

Fig. 11 shows the comparison between the D-BRBF designed for stiff soil and D-BRBF designed for soft soil. It can be observed that the contribution of the MRF within the D-BRBF is higher than 25 %. It can be observed that the two MRF's with different joint typologies have the same behaviour up to a global drift angle of 0.008 rad. With increasing displacement at the top of the building the MRF with CP joints shows an increase in capacity. In comparison with the D-EBF, the D-BRBF evidence a higher deformation capacity. At higher displacements at the top of the building, a small difference can be observed between the D-BRBF with CP joints, and the D-BRBF with RBS joints.

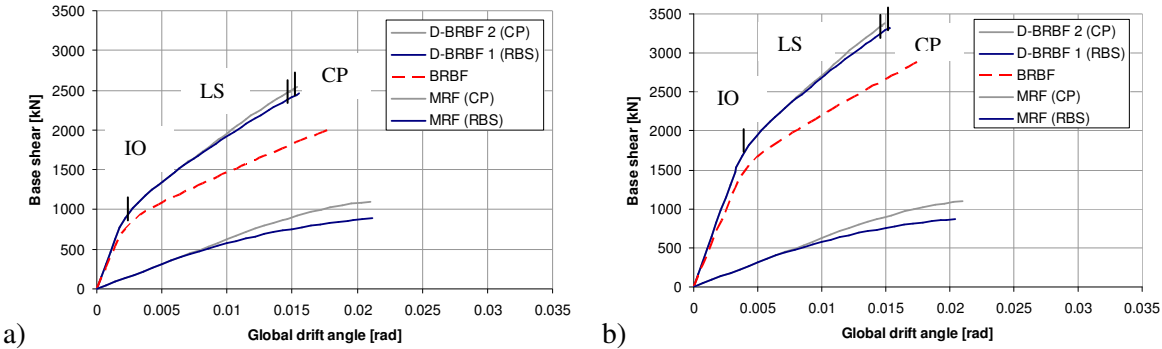


Figure 11. Pushover curves corresponding to the D-BRBF designed for stiff soil a) and for soft soil b)

### 3.3. Incremental dynamic analysis (IDA) on frames

A series of incremental dynamic nonlinear analyses were carried out with the aim to assess the structural performance under seismic loads. For this purpose, each of the eight D-EBF with short links were subjected to a set of ground motion records each scaled to multiple levels of intensity. For each soil type, three accelerograms were chosen from a set of seven ground motion records and used further in the structural analyses. It is to be noted that the ground motion records were scaled so that the design seismic action, characterised by a reference return period of 100 years, corresponds to an intensity level of  $\lambda=1.0$ . The seismic hazard level corresponding to serviceability limit states (SLS) and ultimate limit states (ULS) are related to  $\lambda=0.5$  and respectively  $\lambda=1.5$ .

Fig. 12 shows, for each of the three soft soil records (01, 02 and 03), the inter-storey drift computed for frame 4 at different intensity levels. Considering the ground motion record 02, which lead to the collapse of the structure at  $\lambda=1.6$ , the comparison between the frame 3 with RBS joints and frame 4 with CP joints is shown as well. It can be observed that the behaviour of the two frames is similar until the collapse is reached and the frame with CP joints evidences a slightly higher resistance. Similar to the observations from the pushover analysis, it can be observed also from the incremental dynamic analyses, that the moment resisting frames have a secondary effect.

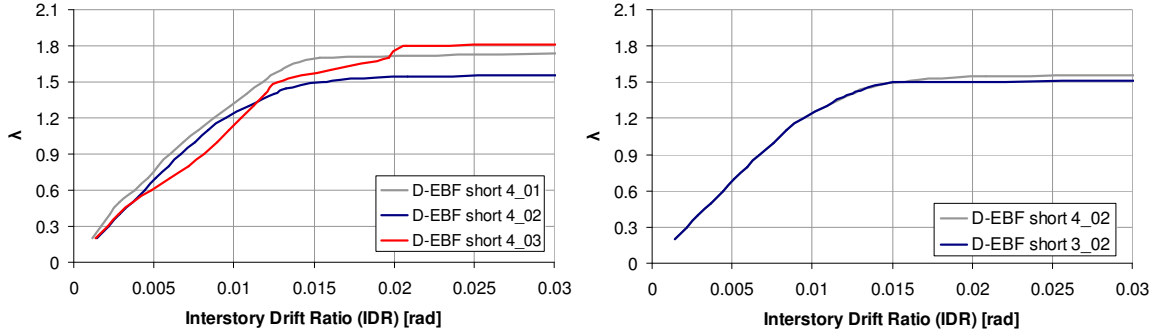
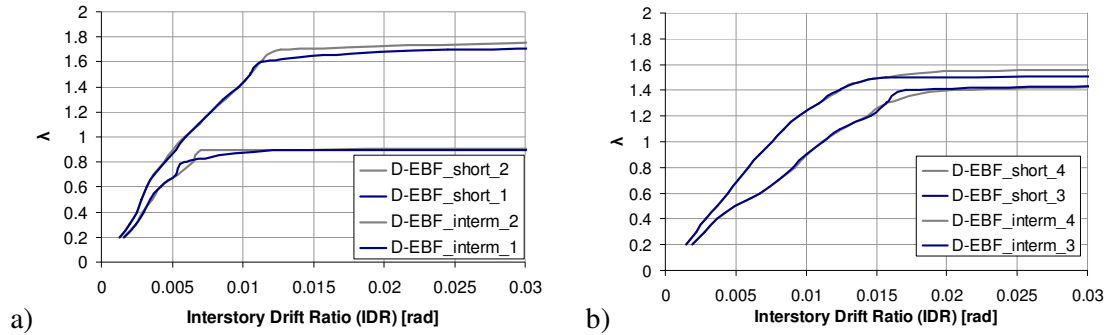


Figure 12. Relative inter-storey drift vs. seismic multiplication factor  $\lambda$  corresponding to D-EBF with short links

The ground motion records “02 for stiff soil” and “02 for soft soil” were used further to assess the seismic performance of the D-EBF frames with intermediate length links, and the performance of the

D-BRBF. Fig. 13a shows the comparison of D-EBF with short links and D-EBF with intermediate links designed for stiff soil. As observed in the pushover analysis, the D-EBF with intermediate links is characterised by a lower resistance. Fig. 13b shows a lower stiffness of the D-EBF with intermediate links than the D-EBF with short links. The frames were analysed in two cases, with RBS and with CP joints. As a consequence, a low increase in resistance can be observed for frames with CP joints.



**Figure 13.** Relative inter-storey drift vs. seismic multiplication factor  $\lambda$  corresponding to D-EBF designed to stiff soil a) and respectively soft soil b)

The results from the incremental dynamic analysis on D-BRBF are shown in Fig. 14a for stiff soil, and in Fig. 14b for soft soil. It can be observed that the interstorey drift ratio is higher for soft soil.

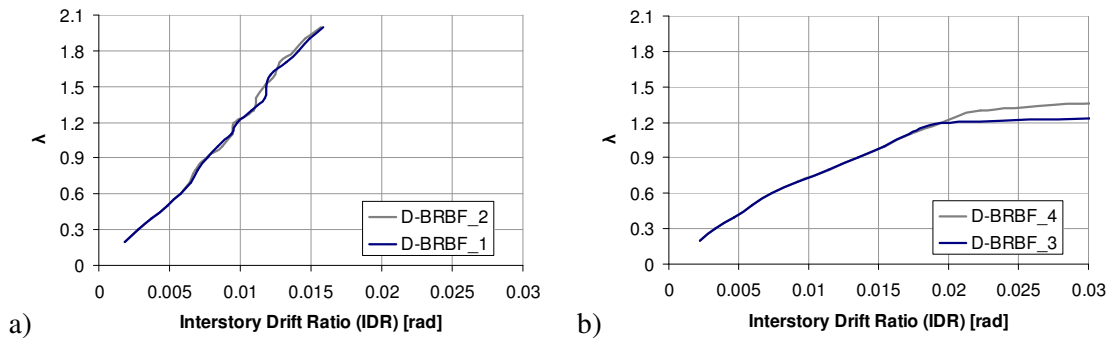


**Figure 14.** Relative inter-storey drift vs. seismic multiplication factor  $\lambda$ , corresponding to D-BRBF designed to stiff soil a), and respectively soft soil b)

Table 3.1. displays the maximum plastic rotation of the short links corresponding to three intensity levels (i.e.  $\lambda=0.5$ ; 1.0; 1.5). Therefore, at  $\lambda=0.5$ , all D-EBF with short links satisfy the immediate occupancy performance level. At and  $\lambda=1.0$ , the frames satisfy the life safety performance level and even the immediate occupancy level. Corresponding to  $\lambda=1.5$ , the frames designed to stiff soil satisfy the life safety performance level, while the frames designed to soft soil reached the collapse.

**Table 3.1.** Plastic rotation in the short links of the D-EBF [rad]

D-EBF short	1	2	3	4	5	6	7	8	
$\lambda$	0.5	0.0145	0.0145	0.021	0.0208	0.0226	0.0226	0.0244	0.0244
	1	0.0624	0.0614	0.0724	0.0726	0.0716	0.0724	0.0786	0.078
	1.5	0.1292	0.1288	***	***	0.1278	0.1298	***	***

Note: extremely large rotations related to failure were observed in the cases marked with \*\*\*

Table 3.2. displays the maximum plastic rotation of the intermediate links corresponding to the three intensity levels (i.e.  $\lambda=0.5$ ; 1.0; 1.5). Consequently, at  $\lambda=0.5$ , all D-EBF with intermediate length links satisfy the immediate occupancy performance level. At and  $\lambda=1.0$ , the frames designed to soft soil, for which the intermediate links have a behaviour closer to short links, satisfy the life safety performance level, while the frames designed to stiff soil reached collapse. Corresponding to  $\lambda=1.5$ , all D-EBF with intermediate links show collapse.

**Table 3.2.** Plastic rotation in the intermediate length links of the D-EBF [rad]

D-EBF interm.	1	2	3	4	5	6	7	8	
$\lambda$	0.5	0.0144	0.014	0.0158	0.0157	0.0127	0.0107	0.0141	0.0137
	1	***	***	0.0627	0.0636	***	***	0.0694	0.0656
	1.5	***	***	***	***	***	***	***	***

Note: extremely large rotations related to failure were observed in the cases marked with \*\*\*

Table 3.3. displays the maximum plastic deformation, developed in the internal core of the BRB, corresponding to the three intensity levels (i.e.  $\lambda=0.5$ ; 1.0; 1.5). For each of the three intensity levels the D-BRBF satisfy the immediate occupancy performance level, with exception of the D-BRBF designed for soft soil that fail at  $\lambda=1.2$  and respectively  $\lambda=1.3$  (see Fig. 14b).

**Table 3.3.** Plastic deformation in BRB [m]

D-CBF BRB	1	2	3	4	
$\lambda$	0.5	0.0048	0.0049	0.0063	0.0063
	1	0.0118	0.0127	0.0269	0.0267
	1.5	0.0183	0.0175	***	***

Note: structural failure was observed in the cases marked with \*\*\* (see Fig. 14b)

The main component of the D-EBF with short links in dissipating the seismic energy is represented by the shear links, while the joints in MRF bays have secondary effect. It was observed that these frames develop plastic hinges mostly in links, and corresponding to higher intensity levels also in joints. An evaluation of the structural behaviour was performed in order to assess their dissipation capacity. The behaviour factor was computed (see Table 3.4.) by  $q=\lambda_u/\lambda_1$ , where  $\lambda_1$  represents the ground motion intensity factor for which the first plastic hinge is developed, while  $\lambda_u$  the factor for which the structure is failing (i.e. the first element reaches the life safety criteria).

**Table 3.4.** Behavior factor overview computed for D-EBF with short links

Frame_Joint	1_RBS	2_CP	3_RBS	4_CP	5_RBS	6_CP	7_RBS	8_CP
HSS / Soil	S460_Stiff		S460_Soft		S700_Stiff		S700_Soft	
$\lambda_{1,avg}$	0.34	0.34	0.36	0.36	0.31	0.31	0.36	0.36
$\lambda_{u,avg}$	1.7	1.7	1.3	1.3	1.67	1.7	1.3	1.3
$q_{avg}$	5	5	3.6	3.6	5.4	5.5	3.6	3.6

In a comparison between the D-EBF with short links and the standard EBF with short links, it was observed that the standard configuration measured a 12% higher inter-story drift ratio than the dual-frame, related to an intensity level of  $\lambda=1.5$ . At serviceability limit state ( $\lambda=0.5$ ), the dual-frame evidenced lower rotation in links than the standard frame. For stiff soil, the rotation reduction in links was 70% at 1st floor, 27% at 2nd floor, 21% at 3rd floor and 12% at 4th floor. For soft soil, the rotation reduction in links was higher, i.e. 11% at 1st floor, 25% at 2nd floor, 67% at 3rd floor and 88% at 4th floor and 300% at 5th floor.

#### 4. CONCLUSIONS

In this study the seismic behaviour of dual frames using HSS was investigated. In particular, two types of soil condition, two high strength steel grades (S460 and S700), and two joint typologies (RBS and CP) were examined within 3 frame typologies, i.e. D-EBF with short links, D-EBF with intermediate links and D-BRBF. A numerical model was calibrated based on results from literature, which allowed assessing the hysteretic behaviour of the RBS and CP joints. Static and dynamic non-linear analyses were carried out.

Corresponding to  $\lambda=0.5$  and  $\lambda=1.0$ , all D-EBF with short links satisfied the immediate occupancy performance level. Corresponding to  $\lambda=1.5$ , the frames designed to stiff soil satisfy the life safety

performance level, while the frames designed to soft soil reached the collapse. Therefore, the soil type has an important influence on the behaviour of the structure. Accordingly, the structural analyses showed a lower performance of the frames located on soft soil than those located on stiff soil. The behaviour factors computed for frames on soft soil were lower than those for frames on stiff soil. This is explained by the fact that ground motions with control period  $T_C$  larger than the fundamental period of vibration of the structure imposed larger ductility demands. Consequently, the behaviour factors recommended in the seismic design codes should be adjusted to account also for the soil condition. A good behaviour was observed for the D-BRBF. The maximum plastic deformation in the BRB at the three seismic hazard levels ( $\lambda=0.5$ , 1.0, and 1.5) was corresponding to the immediate occupancy performance level, with exception of the D-BRBF designed for soft soil which failed at that fail corresponding to a seismic hazard level of  $\lambda=1.2$  and respectively  $\lambda=1.3$ .

Related to the influence of the HSS, it was observed that the frames with CFT of S700 steel grade had a slightly lower stiffness than those with CFT of S460 steel grade. This is justified by the fact that the CFT of S460 steel grade, have a larger cross section. It was observed that the MRF's have a secondary contribution on the behaviour of the dual-frames. Due to the high difference between the stiffness of the EBF and MRF, respectively between BRBF and MRF, the joints develop large plastic deformations only after failure of links, or BRB's. In a comparison between the D-EBF with short links and the standard EBF with short links, related to an intensity level of  $\lambda=1.5$ , it was observed that the inter-story drift ratio of the dual-frame was by 12 % lower compared with the standard frame. At SLS ( $\lambda=0.5$ ), the dual-frame evidenced lower rotation in links than the standard frame.

## ACKNOWLEDGEMENT

The first author was partially supported by the strategic grant POSDRU/88/1.5/S/50783, Project ID50783 (2009), co-financed by the European Social Fund - Investing in People, within the Sectoral Operational Programme Human Resources Development 2007-2013.

The last author was partially supported by the strategic grant POSDRU/89/1.5/S/57649, Project ID 57649 (PERFORM-ERA), co-financed by the European Social Fund – Investing in People, within the Sectoral Operational Programme Human Resources Development 2007-2013.

The present work was supported by the funds of European Project HSS-SERF: "High Strength Steel in Seismic Resistant Building Frames", Grant N0 RFSR-CT-2009-00024.

## REFERENCES

- EN1998-1-1 (2004), Eurocode 8, Design of structures for earthquake resistance - Part 1, General rules, seismic actions and rules for buildings, CEN, European Committee for Standardization.
- P100-1 (2006). Cod de proiectare seismica P100:Partea I, P100-1/2006: Prevederi de proiectare pentru cladiri (in Romanian), 2006.
- EN1994-1-1 (2004), Eurocode 4, Design of composite steel and concrete structures - Part 1, General rules and rules for buildings, European Committee for Standardization.
- Abaqus (2007) Analysis User's Manual I-V. Version 6.7. USA: ABAQUS, Inc., Dassault Systèmes.
- Korotkov V., Poprygin D., Ilin K., Ryzhov S. (2004), Determination of dynamic reaction in concrete floors of civil structures of nuclear power plant in accidental drops of heavy objects, ABAQUS Users' Conference, Boston, 25-27 May, 2004, pp. 399-408.
- Vulcu, C., Stratan, A. and Dubina, D., (2012 - in print), Numerical Simulation of the Cyclic Loading for Welded Beam-To-CFT Column Joints of Dual-Steel Frames, Pollak Periodica.
- Park J.W., Kang S.M., Yang S.C. (2005), Experimental Studies of Wide Flange Beam to Square Concrete-Filled Tube Column Joints with Stiffening Plates Around the Column, Journal of Structural Engineering, Vol. 131, No. 12, December 2005, pp. 1866-1876.
- Dutta A., Dhar S., Acharyya S. K. (2010), Material characterization of SS 316 in low-cycle fatigue loading, Journal of Materials Science, Vol. 45, Issue 7, pp. 1782-1789.
- CSI Berkley, SAP2000 v14.2.2, FAQ (2010).
- FEMA 356 (2000), Prestandard and Commentary for Seismic Rehabilitation of Buildings.
- Bordea S., (2010), Dual Frame Systems of Buckling Restrained Braces – PhD Thesis, Editura Politehnica, Timisoara, ISBN: 978-606-554-059-0.